Photoelectrochemical Approaches for the Conversion of Lignin at Room Temperature

Received 00th January 20xx,
Accepted 00th January 20xx

DOI: 10.1039/x0xx00000x

Shuya Li,[a] Seongsu Park,[a] Benjamin D. Sherman,[b] Chang Geun Yoo[c,d] and Gyu Leem[a,d]*

The selective cleavage of C–C/C–O linkages in lignin represents a key step toward achieving the chemical conversion of this biomass to low molecular weight products under ambient conditions. Photoelectrosynthetic solar cells offer a promising method to address the energy intensive depolymerization of lignin for the production of biofuels and valuable chemicals. While first introducing electrocatalytic approaches to lignin reforming, this feature article gives an in-depth overview of recent progress using dye-sensitized photoelectrosynthtic solar cells (DSPECs) to initiate the cleavage of C–C/C–O bonds in lignin and related model compounds. This approach takes advantage of N-oxyl mediated catalysis in organic electrolyte and presents a promising direction for the sustainable production of chemicals currently derived from fossil fuels.

1 Introduction

Dye-sensitized photoelectrochemical cells (DSPECs) have been studied at a fundamental level for the production of solar fuels—that is, the conversion of water to O_2 and H_2 or the oxidation of water coupled to the reduction of CO_2 for the generation of reduced carbon products. Several research groups have contributed to the development of DSPECs over the last decade with the universal goal of achieving light-driven water oxidation.[1-5] The DSPEC is largely based on the design of a dye-sensitized solar cell (DSSC), first reported in 1991.[6] While employing similar molecule–semiconductor interfaces to achieve light absorption and charge separation, the ability of a DSPEC to carry out net catalysis distinguishes these two classes of solar cells. Progress in generating solar fuels has occurred through improvements to the semiconductor layers,[7, 8] molecular chromophores,[4, 9] and catalysts used.[10, 11] However, DSPECs

[a] Department of Chemistry, State University of New York College of Environmental Science and Forestry, Syracuse, New York 13210, United States.
[b] Department of Chemistry & Biochemistry, Texas Christian University, Fort Worth, Texas 76129, United States
[c] Department of Chemical Engineering, State University of New York College of Environmental Science and Forestry, Syracuse, New York 13210, United States
[d] The Michael M. Szwarc Polymer Research Institute, Syracuse, New York 13210, United States
* Email: gyleem@esf.edu

Shuya Li

Shuya Li obtained her PhD in 2022 at the State University of New York – College of Environmental Science and Forestry under the supervision of Prof. Gyu Leem. Her PhD work focused on the visible-light-driven chemical transformations of biopolymers using dye-sensitized solar cells. In the Fall of 2022, she joined Prof. Weiwei Zheng's group as a Postdoctoral Fellow in the Department of Chemistry at Syracuse University. Her main research interests include performing photocatalysis using perovskite-based semiconductor nanocrystals and the synthesis of solid-state electrolyte for the fabrication of next-generation solar cells.

Seongsu Park

Seongsu Park obtained his BS and MS degrees of Agricultural in 2022 at the Kyungpook National University. Previously his work focused on the modifying low-molar-ratio urea-formaldehyde resins with cellulosic materials. He has currently worked at the Department of Chemistry, State University of New York – College of Environmental Science and Forestry (SUNY ESF) as a Ph.D. student under the guidance of Prof. Gyu Leem. His main research interest is photo-driven chemical transformations of biomaterials using dye-sensitized solar cell.

have yet to demonstrate efficiencies for solar energy conversion to fuel higher than a fraction of a percent.[4, 12] While this might make the application of DSPECs for other important catalytic processes counterintuitive, one need recognize that water splitting presents a daunting challenge to achieve via a photoelectrocatalytic process. Both the thermodynamic (>1.23 eV) and kinetic (four-electron oxidation) requirements of converting water to dioxygen make this a challenging reaction to initiate and sustain at a semiconductor–dye/catalyst–aqueous electrolyte interface.[13] Other catalytic processes, especially ones involving fewer electron counts and/or less thermodynamically demanding reactions, could prove viable for performing with a DSPEC that incorporates semiconductor and molecular components specifically tailored for the targeted chemical reaction(s). With this motivation, Sherman, Yoo, and Leem research groups have developed photoelectrocatalytic processes for oxidative chemical transformations in primary aliphatic and/or benzyl alcohols by combining a DSPEC and aminoxyl radical mediators (ARMs).[14-20]

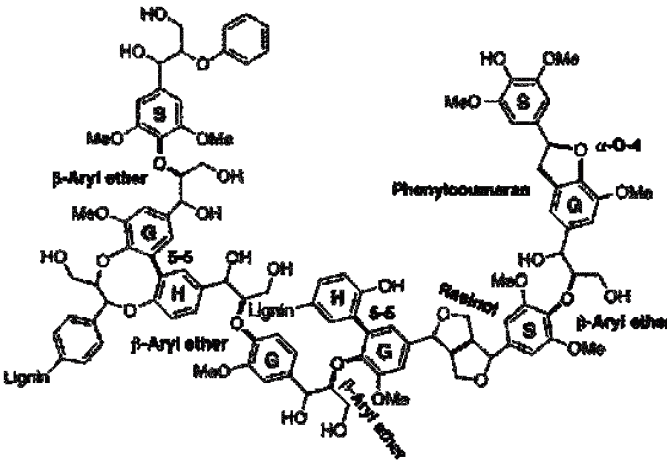

Figure 1. General lignin structure, containing various linkages, including aryl ether (β-O-4, α-O-4), phenylcoumaran (β-5), resinol (β-β), and 5-5, and three primary subunits (S, G, and H units).

Lignin is a three-dimensional amorphous and interlinked biomacromolecule, representing the largest aromatic component in lignocellulosic biomass, and is comprised of three primary monomeric subunits: *p*-hydroxyphenyl (*H*), guaiacyl (*G*), and syringyl (*S*). Interunit linkages mainly consist of the aryl ether (β-O-4, α-O-4), phenylcoumaran (β-5), and resinol (β-β) groups, as shown in the representative structures of native lignin in **Figure 1**.[21, 22] Lignin provides structural integrity and rigidity in plants and helps defend against pathogen attack in nature,[23] while it is a major recalcitrance factor in pulping and biological biofuel conversion processes.[24] Therefore, lignin is typically removed from biomass for effective utilization of carbohydrates like cellulose in traditional biomass-related processes. Unfortunately, the use of the separated lignin has been limited to a combustion energy source in many pulping industries, and only 2% of lignin was further utilized as a surfactant, wood adhesive, or other non-fuel application. Recently, lignin has been intensively studied as an alternative feedstock for petroleum-based platform chemicals

Benjamin D. Sherman

Ben Sherman completed a Ph.D. with Prof. Tom Moore as part of the Gust, Moore, Moore group at Arizona State University in 2013 working on dye-sensitized systems for artificial photosynthesis. After completing a postdoctoral appointment in the lab of Prof. Thomas J. Meyer at the University of North Carolina, he has worked as an assistant professor in the department of chemistry at TCU since 2017. The Sherman research group at TCU pursues the development of photoelectrosynthetic solar cells as a sustainable means for carrying out chemical conversions of economic and industrial interest and for biomass conversion applications

Chang Geun Yoo

Chang Geun Yoo is an assistant professor of chemical engineering at the State University of New York College of Environmental Science and Forestry and an Associate Editor for Frontiers in Chemical Engineering. He has investigated diverse chemistry and engineering approaches in biomass utilization for fuels, chemicals, and materials. His current research focuses on the development of renewable and eco-friendly biorefinery processes by designing an effective solvent system for biomass pretreatment, fractionation, and conversion.

Gyu Leem

Gyu Leem earned a Ph. D. degree in Chemistry from the University of Houston. He is an assistant professor in the department of chemistry at State University of New York College of Environmental Science and Forestry (SUNY ESF) since 2018. Prior to joining the SUNY ESF, he worked as a PostDoc at the University of Florida and a research assistant professor at the University of Texas at San Antonio. He serves as an editorial board member in ACS Applied Nano Materials. His current research interests are focused on the mechanistic pathways for photocatalytic degradation in lignin and lignocellulosic biomass.

and fuels due to its natural abundance, relatively high energy content (~26 kJ/g), and aromatic nature.[25-31] The successful utilization of lignin will generate a new revenue stream for current biorefinery processes and would improve the economic competitiveness of existing cellulose-based product streams. The β-O-4 linkage is the most common recurring linkage between monomeric units (40 - 80% of total linkages) in lignin.[32] The selective cleavage of the C−C and C−O bonds in the β-aryl ether linkage is crucial in facilitating the depolymerization of lignin followed by the production of targeted low molecular weight aromatic compounds.[33, 34] However, the selective cleavage of the C−O and/or C−C bonds in lignin is still a major challenge due to the heterogeneity and complexity of the structure of lignin.

The prospect of using lignin as a renewable and alternative source of aromatic compounds in place of petroleum has motivated several approaches for carrying out lignin depolymerization. Over the last few decades, diverse lignin conversion strategies have been intensively investigated for producing value-added products including thermal (e.g., pyrolysis,[35-37] gasification[38, 39]), reductive,[40, 41] and oxidative cracking methods.[42-44] Thermal degradation approaches can readily decompose lignin to bio-oil at elevated temperatures (400–600 °C), however, this approach faces fundamental problems including low selectivity of aromatic products and unwanted water and char formation.[45, 46] The reductive conversion approach degrades and transforms lignin via hydrogenolysis, hydrodeoxygenation, and hydrogenation with a redox catalyst and hydrogen donors. This method is relatively selective for the production of aromatic compounds, but reliance on noble-metal catalysts (e.g., Pt, Ru, Pd) and hydrogen gas has motivated the search for effective inexpensive transition-metal catalysts (e.g., Ni, Fe, Cu) and other hydrogen sources (e.g., hydrogen donor solvents) to avoid limitations related to transportation and storage of hydrogen gas.[47] Oxidative cracking is the alternative approach which targets hydroxyl groups of lignin. This approach requires relatively mild reaction conditions. However, conventional thermochemical oxidation methods lead to uncontrollable side reactions resulting in diminished selectivity and efficiency for the production of the targeted aromatic compounds.[48] For instance, direct C−C bond cleavage of in lignin requires elevated temperature (e.g., 80 °C) and extended periods (>40 h) which leads to the low selectivity (less than 60%) of cleavage products via a homogeneous catalysis system (**Figure 2a**).[49, 50] Recently, direct electrocatalytic,[51-54] photocatalytic methods,[16, 33, 55] or the combination of electrocatalysis and photocatalysis[56, 57] have been developed for efficient lignin decomposition. For example, we recently reported the photocatalytic cleavage of C−C and C−O bonds at room temperature using dye-coated TiO_2 nanoparticles (**Figure 2b**).[16] Polypyridyl ruthenium complexes containing carboxylic acid moieties immobilized on TiO_2 nanoparticles were used as a photocatalyst to perform oxidative cleavage of a phenolic lignin model compound in acetonitrile solution.[16]

The catalytic cleavage of the C−O and C−C linkages in lignin has remained a scientific puzzle for both industrial and academic scientists. For example, the $C(sp^3)$−$C(sp^3)$ bond is quite stable at

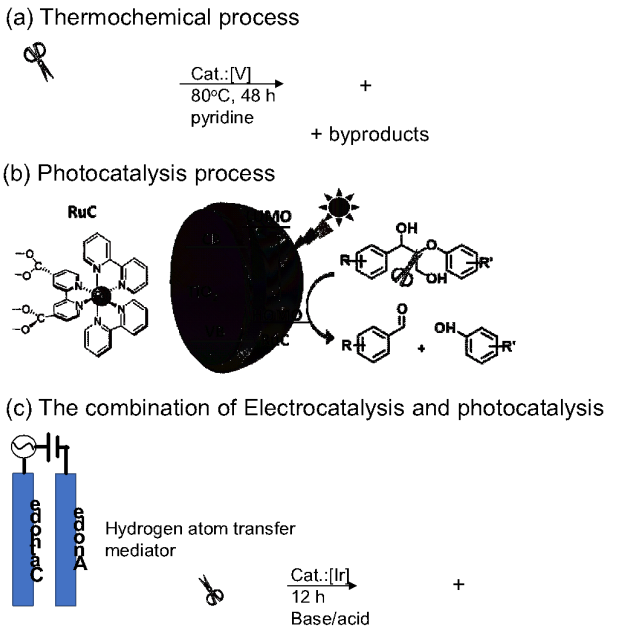

Figure 2. General lignin oxidative cleavage strategies and characteristics. (a) Thermal catalytic cleavage strategy. (b) Photocatalytic process. Reprinted with permission from reference 16. Copyright 2022 American Chemical Society. (c) Electrocatalytic oxidation and photocatalytic reductive cleavage in a two-step process.

room temperature, with a bond dissociation enthalpy (BDE) of 69.2 kcal/mol.[57, 58] Thus, a photochemical lignin degradation strategy using a two-step process (peroxidation followed by the aryl ether linkage cleavage) was introduced to address the aforementioned challenges.[1, 56, 57] Nguyen *et al.* reported that the photocatalytic depolymerization method exhibited controllable lignin decomposition reactions by utilizing a two-step oxidation/reduction method.[57] This method first activated lignin to weaken the bond dissociation energy of C−O bonds and then cleaved the C−O bonds at room temperature using the photocatalysts. Luo *et al.* also introduced the photocatalytic degradation of lignin using porous organic polymers with stepwise oxidation and reduction.[59] The Stephenson group has reported a highly selective two-step—alcohol oxidation followed by reductive cleavage—depolymerization of native lignin at ambient temperature via electrochemical and photochemical approaches (**Figure 2c**).[57]

According to the Web of Science (September 2022), a key word search of scientific publications with “lignin” and either “electrocatalysis” or “photocatalysis” returns 236 hits. The network map with the keyword analysis results by the full counting method via VOSViewer [60] is presented in **Figure 3**. As the network map indicates, lignin research has mainly been conducted with photocatalysis for deconstruction purposes with the keywords “depolymerization", "photodegradation", "conversion", and "cleavage” closely associated. Moreover, the map indicates that lignin oxidation is the main degradation reaction in terms of photocatalysis. Very recently, we reported on the oxidative photoelectrochemical transformation of lignin under mild condition.[20] This photoelectrocatalytic oxidation

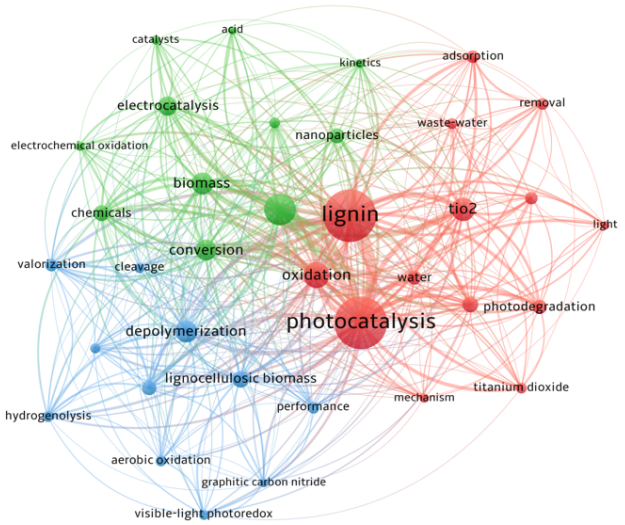

Figure 3. The network map with keyword co-occurrence in scientific publications on "lignin" with either "electrocatalysis" or "photocatalysis" searched by Web of Science.

process leads to enhanced selectivity and effective chemical transformations of aliphatic and/or benzylic alcohols under ambient conditions.[14, 15, 19, 20] Our recent work on developing DSPEC processes incorporating ARMs for achieving benzyl alcohol oxidations and lignin degradation will be discussed later. The photoelectrocatalytic mechanisms and the key mechanistic pathways of chemical transformation for solar or visible light driven lignin degradation will also be considered.

2 Electrocatalytic Approaches to Chemical Oxidations

Electrocatalytic oxidation methods provide controlled tuneable approaches to lignin degradation under galvanic conditions.[54, 61] The direct electrochemical transformation of lignin in which C−O and/or C−C bonds were cleaved has been reported.[62] This approach requires applied bias (e.g., 1.45 V vs SCE) to drive the reaction.[63] The morphology and surface structure of the anode alloy used (e.g., Ni, Co, Fe) need to be considered as most lignin oxidation occurs by adsorption on the surface of the anode. In comparison to this direct electrooxidation process, aminoxyl radical mediated electrochemical oxidation enables similar types of lignin conversion. Using this mediated electrochemical approach can significantly reduce the necessarily applied potential and lead to excellent chemoselectivity of the products formed by lignin depolymerization at room temperature.[64] In the indirect mediator-assisted electrocatalytic oxidation of lignin, the mediator provides an easy route for proton/electron transfer from the electrode/electrolytic solution to target lignin oxidation sites.

The aforementioned electrocatalytic and photocatalytic methods were widely investigated for selective C−O and C−C bond cleavage in lignin. Examples, as shown in **Figure 4**, include electrocatalysis coupled with an oxidizing agent that was used

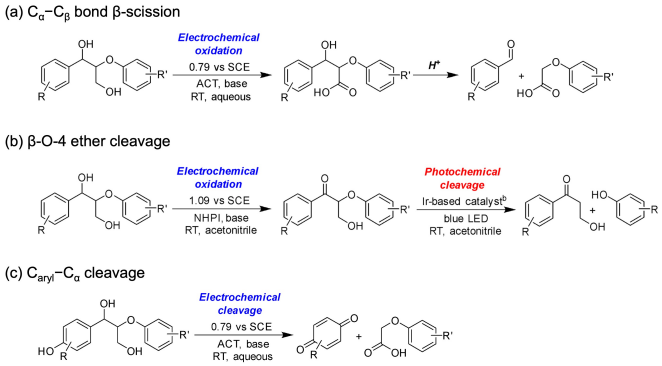

Figure 4. Selective examples of C−O and/or C−C bonds cleavages: (a) C_α–C_β bond cleavage, (b) C_β–O ether bond cleavage, and (c) C_{aryl}–C_α bond cleavage. The recently developed redox methods in mild conditions are present in red for photochemical methods and in blue for electrochemical strategies.

for C_α–OH or C_γ–OH oxidation as the first step for selective C_β–O or C_α–C_β cleavage (**Figures 4a and 4b**).[56, 64] As for photo-induced lignin conversion, Ir-based photocatalysts were used for the reductive cleavage of C_β–O bonds (**Figure 4b**).[56] Additionally, 4-acetamido-2,2,6,6-tetramethylpiperidine N-oxyl (ACT)-mediated electrolysis was reported to effectively cleave the C_{aryl}–C_α bond with ~ 45% yield of two major cleavage products, 2,6-dimethoxybenzoquinone (52%) and 2-(2-methoxyphenoxy)acetic acid (36%) as shown in **Figure 4c**.[64] ACT-mediated electrocatalytic approaches allow for excellent control over the reaction and thus high yields of the resulting products. Therefore, these methods are considered cost-effective and 'green' processes and present an attractive approach for industrialized valorisation.

3 Photoelectrochemical oxidation approaches

Photoelectrochemical (PEC) approaches to artificial photosynthesis build of the concepts of electrocatalysis and photocatalysis. While electrocatalytic lignin oxidation generally requires high applied overpotential and exhibits low product selectivity, PEC approaches require more mild applied bias conditions and has been shown to promote good selectivity for product formation. In comparison with colloidal photocatalytic systems, PEC approaches using heterogeneous electrode interfaces enable easy recovery of the light absorber and (if surface immobilized) of the co-catalyst. Moreover, back-side illumination of the transparent conducting oxide substrates used to fabricate PEC photoelectrodes addresses one of the biggest challenges of colloidal photocatalysis in dark-colored lignin solutions where light does not penetrate into solution, resulting in low photocatalytic efficiencies. Generally performed under mild ambient conditions, PEC solar cells capture and convert solar energy into stored energy in the form of chemical fuels, such as hydrogen gas (equation 1) or reduced carbon-based fuels (*i.e.,* methanol, equation 2).[65-67]

$$2H_2O \rightarrow 2H_2 + O_2 \quad \textbf{(1)}$$

$$2H_2O + CO_2 \rightarrow CH_3OH + O_2 \quad \textbf{(2)}$$

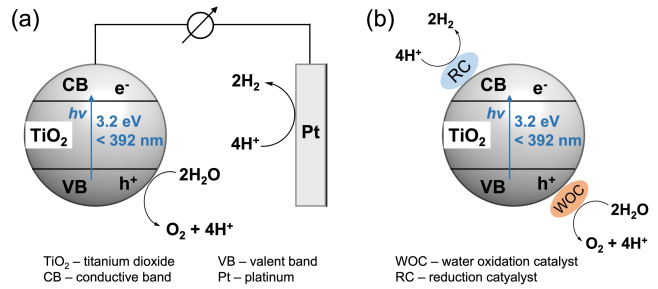

Figure 5. (a) The Honda-Fujishima photoelectrochemical cell with TiO_2 as a photoanode. (b) Illustration of a single semiconductor nanoparticle with the water oxidation catalyst and the reduction catalyst.

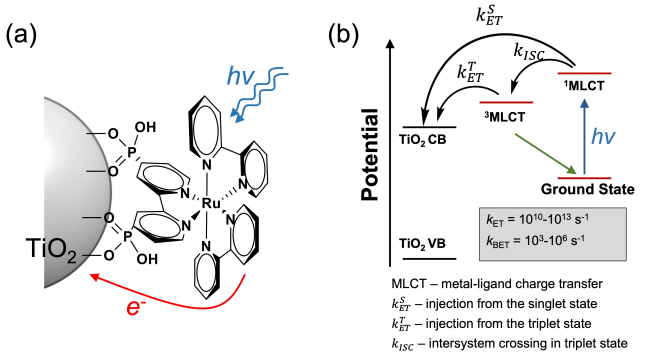

Figure 6. (a) Illustration of a Ru-based chromophore and semiconductor assembly. (b) Photodynamics of the Ru(II) chromophore on a TiO_2 surface, electron injection from a singlet state and a triplet state into the conductive band, and back electron transfer to oxidized Ru^{3+}.

A first demonstration of solar water splitting was described by Honda and Fujishima which used ultraviolet (UV) bandgap excitation of an anatase titanium dioxide (TiO_2) photoanode.[68] In **Figure 5a**, direct 3.2 eV bandgap excitation of TiO_2 generates oxidizing holes (h^+) at the TiO_2–electrolyte interface and mobile charge carriers at the conduction band (CB) potential following charge separation. Researchers have also performed water splitting with colloidal TiO_2 nanoparticles decorated with surface loaded water oxidation catalysts (WOC) and hydrogen evolution reaction (HER) catalysts (see **Figure 5b**).[69] In this way, charge separation occurs from TiO_2 to different catalysts. However, rapid charge recombination and back electron transfer (BET) still exist and impact the light conversion efficiency.[70, 71]

Given the limited flux of UV photons at ground level, the use of TiO_2 as the primary light absorber greatly limits the potential efficiency of the PEC system. Efforts to extend light absorption to visible wavelengths with oxide semiconductor-based absorbers include the use of doped TiO_2 materials[72-75] and the use of other oxides with suitable band alignments and band gaps in the visible range such as $BiVO_4$,[76] Fe_2O_3,[77] WO_3,[78] and others.[79] An alternative approach to the use of a direct band gap absorber is to increase the light absorption range of a TiO_2-based electrode with an immobilized monolayer surface coating of a molecular dye. As mentioned earlier, PECs using this type of electrode are referred to as dye-sensitized photoelectrochemical cells (DSPEC).[80-83]

Metal complex or complex ion chromophores have been widely used in DSPECs for water splitting or CO_2 reduction due to their excellent photophysical properties.[84] Ruthenium(II) tris-bipyridine (bpy), $[Ru(bpy)_3]^{2+}$, is one of the conventional metal-based chromophores used in DSPECs due to its wide light absorption range from near-UV to visible light, the high chemical stability of the metal-to-ligand-charge-transfer (MLCT) excited state, and the high potential of the $Ru^{3+/2+}$ couple ($E'_{1/2} \cong 1.4$ V vs. NHE).[85-87] For example, Ru chromophores containing anchoring moieties (e.g.,. phosphonate or carboxylate groups) covalently bond to semiconductor oxide surfaces.[88] While the phosphonate anchoring groups form a more robust linkage to TiO_2, carboxylate surface anchored Ru chromophores show higher electron injection efficiency.[89] The scheme in **Figure 6a** shows a phosphonate anchor group containing $[Ru(bpy)_3]^{2+}$ chromophore on a TiO_2 nanoparticle. **Figure 6b** outlines the photodynamic steps initiated upon excitation of the Ru chromophore.[90-92] Marcus-Gerischer theory indicates that injection from the initial ^{1}MLCT state occurs at the femtosecond timescale. Alternatively, injection from the lowest ^{3}MLCT state occurs on the picosecond timescale. A sufficiently positive applied bias to the DSPEC photoanode serves to drive charge collection at the ohmic contact and limits back electron transfer (BET) to surface oxidized chromophores.[93, 94]

The use of dye-sensitized photoanodes in photovoltaic solar cells (i.e., DSSCs) represents a mature technology.[6, 82] However, recent DSSC related research has targeted improved overall solar conversion efficiencies through the development of novel dye structures and redox mediator species.[95-97] In the context of photoelectrosynthetic solar cells (where a photoelectrosynthetic cell is a type of PEC that performs overall endothermic cell chemistry), Treadway *et al.* first described the use of a $[(4,4'\text{-}(CO_2H)_2bpy)(4,4'\text{-}Me_2bpy)Ru(II)(dpp)Ru(II)(tpy)(OH_2)]^{4+}$ ($4,4'\text{-}(CO_2H)_2bpy$ = 2,2′-bipyridine-4,4′-dicarboxylic acid; $4,4'\text{-}Me_2bpy$ = 4,4′-dimethyl-2,2′-bbipyridine; dpp = 2,3-bis(2-pyridyl)-pyrazine; tpy = 2,2′:6′,2″-terpyridine) complex adsorbed on a mesoporous nano-structured TiO_2 electrode for the conversion of 2-propanol to acetone.[98] The first demonstration of a dye-sensitized photoanode capable of driving the water oxidation half reaction was reported in 2009 through a collaboration of the Mallouk and Gust, Moore, Moore research groups.[99] This first report used a modified $[Ru(bpy)_3]^{2+}$ dye containing separate bipyridine ligands, one with phosphonic acid groups (for adsorption to the TiO_2 surface) and another with a malonic acid functional group for binding to colloidal $IrO_2 \bullet nH_2O$ nanoparticles which served as the water oxidation catalyst. The development of dye-sensitized photoanodes for water oxidation progressed rapidly after this first report with notable improvements including the development of [(2,2′-bipyridine-6,6′-dicarboxlyate)L_2Ru(II)]-type catalysts (Ru(bda), L usually an N-cyclic aromatic ligand),[10, 100, 101] the use of core-shell electrode surfaces,[7, 8] and methods for stabilizing the photoanode surface.[102, 103] Several review articles offer comprehensive and in-depth overview of this research which is outside the scope of the present discussion.[4, 11, 65, 104-106]

4 Aminoxyl mediated photoelectrochemical oxidation approaches

Combining the concepts of mediated electrocatalysis, especially in the context of C—C or C—O bond cleavage of lignin, with that of dye-sensitized photoelectrochemical cells has given rise to aminoxyl mediated DSPECs for biomass conversion or alcohol oxidation in non-aqueous media.[15, 19, 20] Work related to the development of this specific type of DSPEC will be discussed below, and the later sections will give a detailed review of the recent work related to lignin conversion and mechanistic pathways.

PEC Alcohol oxidation. As mentioned above, one of the first reports for a non-regenerative photoelectrochemical cell utilizing a dye-sensitized photoanode demonstrated the viability of this approach through the conversion of 2-propanol to acetone.[98] While much of the focus in developing DSPECs has centered on overall water splitting, several studies have tested dye-sensitized photoanodes in the context of driving organic oxidations, whether as a sacrificial chemical stand-in for water oxidation or as the targeted chemistry outright. For instance, light driven hydroquinone oxidation has been used to test the photocurrent activity of organic-dye sensitized photoanodes[107] and served as a half reaction coupled to hydrogen production in a tandem DSPEC system.[108] In a similar way, triethanolamine (TEOA), ethylenediaminetetraacetic acid (EDTA), and nicotinamide adenine dinucleotide (NADH) have been used as irreversible sacrificial donors to better understand the photodynamics in the context of DSPECs.[109, 110]

Efforts in purposefully driving targeted organic conversions photoelectrochemically with dye-sensitized photoanodes has extended from the observed catalytic ability of $[Ru(tpy)(bpy)(OH_2)]^{2+}$ and related Ru(II) complexes for driving organic oxidations in aqueous solution.[111, 112] In this direction, Pho *et al.* studied the activity of a terthiophene–$[Ru(tpy)(bpy)(OH_2)]^{2+}$ dyad attached via phosphonic acid linker to TiO_2 for the light driven oxidation of phenol and benzyl alcohol.[113] With either substrate, photochemical activation of the Ru center to the Ru^{IV}=O state preceded alcohol oxidation. High photocurrents in the presence of phenol implied a faster rate of catalysis compared with benzyl alcohol. Stable long-term photocurrents were observed with both substrates, and the addition of 4-*tert*-butylpyridine noticeably improved the long-term photocurrent stability with benzyl alcohol substrate under the pH 4.35 acetate buffered conditions of the study. Following up on this work, Jiang *et al.* reported a chromophore–catalyst assembly on mesoporous TiO_2 electrodes for carrying out phenol and benzyl alcohol oxidation in aqueous solution.[114] In this case, the surface assembly featured a $[Ru(phenq)(tpy)]^{2+}$ (phenq = 2-(quinol-8′-yl)-1,10-phenanthroline) catalyst, and as opposed to a surface immobilized dyad complex, the chromophore ($[Ru(bpy)_3]^{2+}$) and catalyst centers were connected via a polystyrene backbone and the polymeric assembly deposited on the photoanode surface using a layer-by-layer (LbL) self-assembly method. Increasing photocurrents under mild applied bias (0.2 V vs. Ag/AgCl) in response to increased concentrations of phenol and benzyl alcohol demonstrated the viability of this poly-electrolyte LbL approach for establishing DSPEC photoanode surfaces as an alternative to the use of acid anchoring groups.

Using co-immobilized phosphonic acid derivatives of the $[Ru(bpy)_3]^{2+}$ chromophore (RuP) and $[Ru(Mebimpy)(bpy)(OH_2)]^{2+}$ catalyst (Mebimpy = 2,6-bis(1-methylbenzimidazol-2-yl)pyridine), Song *et al.* demonstrated overall benzyl alcohol dehydrogenation (eqn. 3) using a DSPEC.[115] As opposed to just studying the anodic half reaction (alcohol oxidation), this approach illustrates how a DSPEC could be leveraged to produce two value added products (benzaldehyde and molecular hydrogen) from a low value precursor (benzyl alcohol). While requiring an applied bias of 0.2 V vs. NHE (pH 4.5 acetate buffered electrolyte), the production of benzaldehyde and hydrogen gas products were verified with faradaic efficiencies of 26% and 87%, respectively. Recent work by Badgurjar *et al.* has elaborated on this approach using the same Ru(II) catalyst but with a BODIPY-based (boron dipyrromethene) molecular light absorbers on SnO_2@TiO_2 electrode surfaces.[116] While supporting low overall efficiency for the photoelectrolysis of benzyl alcohol, this work does show the inherent flexibility of DSPECs for tuning the light absorbing properties of the photoanode surface, with the BODIPY dyes extending light absorption to wavelengths longer than 650 nm.

$$PhCH_2OH \rightarrow PhCHO + H_2 \quad \textbf{(3)}$$

Each of the studies mentioned above used a Ru(II) based complex as the catalyst to facilitate the photo-driven oxidation of the organic substrate (i.e., benzyl alcohol). As remarked earlier, aminoxyl radicals also serve as effective catalysts for controlled alcohol oxidations.[117] Recent studies have examined the utility of coupling bismuth vanadate, a 2.4 eV bandgap n-type semiconductor, with N-oxyl mediators to achieve specific organic oxidations such as the conversion of 5-hydroxymethyfurfural (HMF) to 2,5-furandicarboxylic acid (FDCA) with TEMPO[118, 119] or the formation of 1-tetralone from tetralin mediated by N-hydroxysuccinimide (NHS).[120] Specifically in the case of benzyl alcohol oxidation, $BiVO_4$-based photoanodes, both with NHS[120] and TEMPO,[14] have demonstrated the production of benzaldehyde with faradaic efficiencies of ≥85%. This reaction has also been the focus of dye-sensitized photoanode based systems relying on TEMPO to mediate the production of benzaldehyde both with the TEMPO dissolved in the electrolyte[121] and with surface bound chromophore–TEMPO dyad or triad type surface adsorbates.[122] These studies highlight recent efforts in developing photoelectrosynthetic solar cells for the production of fine chemicals and hydrogen fuel that complement our work described in the sections below targeting the photoelectrochemical conversion of lignin.

Secondary benzyl alcohol oxidation. According to previous studies,[33, 42, 56, 57] a two-step process (selective preoxidation followed by aryl ether linkage cleavage) has proven to be an efficient means for the production of aromatic products from lignin. This section describes the photocatalytic oxidation of the C_α–OH as the initial step of photocatalytic cleavage of the β–O–4 linkages in lignin according to our recent study.[20] The C–O bond dissociation energy of the β–O–4 linkage can be significantly reduced upon the oxidation of the α- or γ-carbon.[56, 58] Our previous work demonstrated the oxidation of alcohols (*e.g.,* phenol and benzyl alcohol) using a Ru-polypyridyl based catalyst adsorbed onto a TiO_2 electrode in aqueous solution.[113,

[114] The observation that Ru-polypyridyl complexes are reactive with respect to organic oxidations in aqueous media has led to the focus here on solar light-driven chemoselective oxidation (*e.g.,* 2° benzylic alcohol oxidation) experiments using a lignin model compound in a DSPEC under mild conditions. To probe light driven electron transfer between RuC and *N*-hydroxyphthalimide (NHPI), as well as the ability of the oxidized NHPI to catalyze the formation of a C_α-ketone from a lignin model compound, photocurrent current experiments were conducted as shown in **Figure 7a**. TiO_2-RuC photoanodes were measured in acetonitrile electrolyte with on/off illumination cycling using a 200 mW cm^{-2} AM 1.5G light source. Under an applied bias of 0.75 V vs. SCE, the photocurrent in the presence of NHPI and Model-ol (green trace in **Figure 7b**) significantly exceeds that without the co-catalyst, NHPI/2,6-lutidine (LTD), or the light illumination present in solution (red trace in **Figure 7b**). The enhanced photocurrent in the presence of NHPI, as well as the sustained photocurrents under illumination, indicate that RuC can support light-driven oxidation to form the N–O$^\bullet$ radical, which can subsequently carry out HAT with Model-ol.

To investigate if Model-one was in fact the product of the photocurrent activity, a 20-hour continuous illumination experiment using the above described conditions was performed and the species present in solution monitored by gas chromatography and ^{1}H NMR. Based on the results, an >90% conversion of Model-ol to Model-one was obtained over the 20 h experiment, with less than 10% conversion observed during the same time length with no illumination or with illumination but no NHPI/LTD co-catalyst present in solution (**Figure 7c**). The faradaic efficiency (FE) was calculated to be 78% with ~4 C of charge consumed during the 20 h illumination. This DSPEC system was also applied to veratrylglycerol-β-guaiacyl ether model compound which closely resembles the structure of the β-aryl ether linkage in natural lignin. According to the results of 2D heteronuclear single quantum coherence (HSQC) NMR analysis, the contour of the β-position of the linkage was remarkably shifted, consistent with oxidation of the C_α, with a >70% conversion yield of C-OH to C=O and a FE of 72%. This indicates that the PEC can effectively and selectively oxidize the hydroxyl group at α-position of the model compound (**Figure 7d**). These results provide strong evidence for the viability of a PEC to perform lignin decomposition via sequential oxidative and reductive photocatalytic C–O bond cleavage.

Selective oxidative cleavage of C_{aryl}–C_α in a phenolic lignin model compound (LMC). Selective cleavage of C−C/C−O bonds is a useful chemical transformation in organic synthesis and chemical industry. This chemical transformation can be used for the depolymerization of biomacromolecules (*e.g.,* lignin) because a C−C/C−O bond is one of the main targeted linkages to be cleaved in lignin.[123] Among the C−C/C−O bond cleavages, the direct cleavage of C_{aryl}–C_α generally requires a high temperature (e.g., 80 °C) and long reaction periods (> 40 h).[50, 124] For example, metal-based catalysts (e.g., copper (Cu)[141] or vanadium (V)[73]) were investigated for selective C−C bond cleavage in lignin substrates. Interestingly, the cleavage reaction pathways are dependent on the presence of phenolic moieties in lignin. Our recent study reported visible light driven heterogeneous photocatalytic C_{aryl}−C_α bond cleavage with a phenolic lignin dimer at room temperature.[19] This study focused on the photocatalytic oxidative cleavage of the C_{aryl}−C_α (β-O-4 of aryl

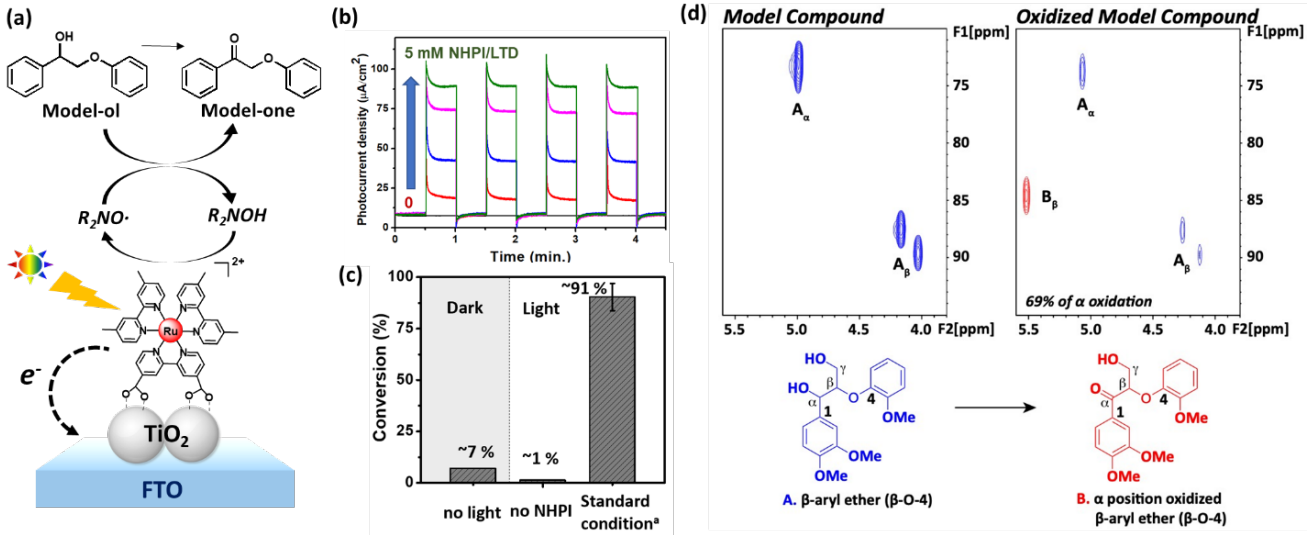

Figure 7. (a) Schematic of photocatalytic conversion of lignin model compound in a DSPEC-LC. (b) Photocurrent−time traces at TiO_2-Ru films with increasing the N-hydroxyphthalimide (NHPI) and 2,6-lutidine (LTD), 0 (red), 1.5 (blue), 3 (pink) and 5 (green) mM each with control group performed by bare TiO_2 (black) films with 30 s light off/on cycles in 0.1 M tetrabutylammonium hexafluorophosphate ($TBAPF_6$), 2.5 mM 2-phenoxy-1-phenylethanol (Model-ol) in acetonitrile; E_{appl} = 0.4 V. Illumination with 200 mW·cm^{-2} visible light, λ > 400 nm. (c) Conversion of photocatalytic oxidation of lignin model compounds with and without NHPI/LTD pair and light illumination. [a]Standard condition: Model-ol (2.5 mmol), LTD (5 mmol), and NHPI (5 mmol) under the illumination (AM1.5G, 2 sun, 200 mW cm^{-2}) with an applied bias of 0.4 V versus Ag/Ag^+. (d) 2D HSQC NMR spectra of veratrylglycero-β-guaiacyl ether model compound before and after photocatalytic oxidation in the DSPEC-LC system. Reprinted with permission from reference 20. Copyright 2020 American Chemical Society.

ether linkage) bonds by using a designed TiO_2 nanorod array (TiO_2 NRA) type PEC incorporated with an aminoxyl radical mediator (ARM-PEC). Our recent publications have detailed the use of both mesoporous and nanorod-based TiO_2 photoanodes modified with RuC (TiO_2-RuC) and shown high photocurrents and excellent conversion efficiencies with ACT or NHPI for generating oxidized LMC products.[15, 19, 20] To prove electron injection of photoexcited RuC* to TiO_2 and hole transfer of RuC to ACT, the electrochemical and photoelectrochemical measurements were conducted with a TiO_2-RuC photoanode, ACT, and a phenolic LMC. As displayed in **Figure 8**, the TiO_2-RuC in a neat electrolyte shows a characteristic redox couple (black voltammogram, $E_{1/2}$ = 1.09 V vs Ag/Ag^+) for the surface-bound $RuC^{III/II}$. Upon the addition of ACT, a new wave with a pronounced cathodic onset starting at approximately 0.3 V vs Ag/Ag^+ was observed (red voltammogram), indicating a diffusional character. Then, the steady-state current occurred at potentials > 0.7 V vs Ag/Ag^+ attributed to the oxidation of ACT to the oxoammonium species ACT^+. The addition of LMC with ACT in solution introduces a strong catalytic wave with the formation of the ACT^+ species (blue voltammogram). On the basis of these results, the direct electrochemical activation of this catalytic process occurs at a higher applied bias (> + 0.4 V vs. Ag/Ag^+). Thus, the photochemical behavior of the TiO_2-RuC photoanode was carried out at more negative applied bias (+ 0.1 V vs Ag/Ag^+) under illumination with visible light (1 sun) indicating effective photocatalytic activation of the DSPEC system shown in **Figure 8b**. The photocurrent with increasing concentration of ACT exceeds 190 μA cm^{-2} (green), indicating that RuC can support light-driven oxidation of ACT to form the ACT^+ by RuC(III), and then reforming the ground state RuC(II) upon light absorption and electron injection from RuC to the conduction band of TiO_2 (**Figure 8c**). These results provide strong evidence for the viability of a PEC to perform the targeted chemical transformation in lignin via photocatalytic selective C–C bond cleavage at low applied potentials under ambient conditions. A 5-hour continuous illumination experiment was performed with the photoanode under 1 sun condition in the presence of the ACT and LMC under ambient conditions. The species present in the solution were monitored by gas chromatography FID, GC-MS, NMR, and 2D heteronuclear single quantum coherence (HSQC) NMR analysis. Based on the results, an excellent selectivity > 91% from LMC to selective C_{aryl}-C_α cleavage products was obtained and confirmed by 2D HSQC NMR (**Fig. 8d**). The photoexcited RuC photocatalyst activates an ACT to catalyze the oxidative cleavage of C_{aryl}-C_α in a phenolic lignin dimer generating two cleavage products 2-(2-methoxyphenoxy)acrylaldehyde (88%) and dimethoxybenzoquinone (95%) (**Figure 8e**), with a FE of 79%. Based on interfacial dye loading, a high photo-turnover number (PTON) was observed (>3000) for this system, which indicates the high efficiency of PEC-induced lignin conversion**.** Interestingly, the LMC plays the important role of a sacrificial

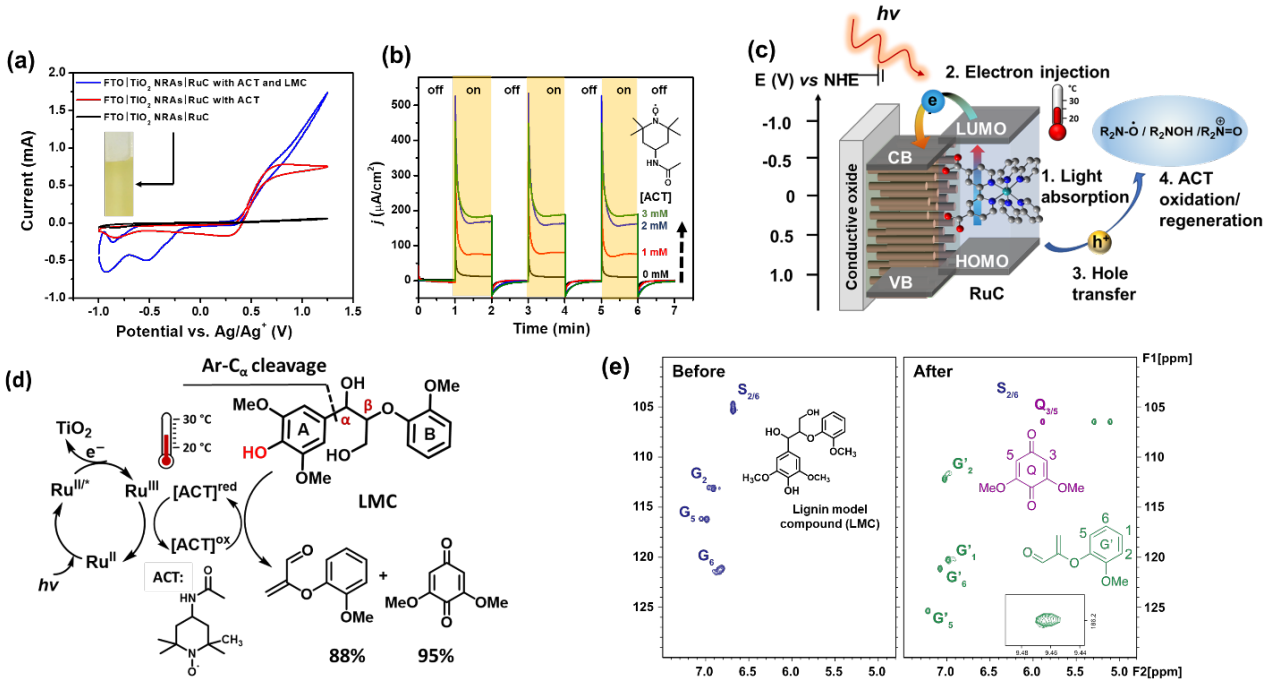

Figure 8. (a) CVs of FTO/TiO_2-RuC films (black), the same with ACT (red), and both ACT and a lignin model compound (LMC) (blue). (b) Photocurrent–time traces at FTO/TiO_2-RuC films with increasing concentration of the ACT, 0 (black), 1 (red), 2 (blue) and 3 (green) mM each with control group performed by the films with 60 s light off/on cycles in 0.1 M tetrabutylammonium hexafluorophosphate ($TBAPF_6$) in acetonitrile; E_{appl} = 0.1 V vs Ag/Ag^+. Illumination with 100 $mW \cdot cm^{-2}$ visible light. (c) Schematic for the visible light induced charge transfer between surface bound RuC and ACT in a PEC. (d) Proposed mechanism for photocatalytic oxidative cleavage of LMC. (e) Aromatic regions of 2D HSQC NMR spectra of the LMC before and after photoelectrocatalytic reactions in the DSPEC system. Reprinted with permission from reference 19. Copyright 2021 American Chemical Society.

mediator in a DSPEC system.[19, 20] This system showed excellent photocatalytic activity to facilitate controlled selective bond cleavage of C–C/C–O bonds without additional heat energy or high applied potential bias. The possible reaction pathways for the oxidative bond cleavage in a photoelectrochemical cell follows a series of photodynamic events: (1) photoexcitation of the surface-bound Ru(II) photocatalysts, (2) electron and hole generation (TiO_2(e-) and Ru(III), respectively) following electron injection into TiO_2 NRAs, (3) electron transfer from ARM to Ru(III), (4) formation of oxidized ARM^+ that should activate HAT-mediated oxidative cleavage of lignin substrates, and (5) the intramolecular proton transfer for a direct C−C or/and C−O bond cleavage (depending on a hydrogen atom transfer mediator) and ARM catalyzed dehydration to produce aromatic compounds. The oriented one-dimensional TiO_2-NRA with controllable porosity has exhibited great performance with regards to electron transport in dye-sensitized solar cells.[125, 126] In comparison with randomly packed mesoporous TiO_2 films, the TiO_2 NRAs are perpendicular to the substrate which enables faster electron/hole transport and slower charge recombination.[127] Our recent studies exhibited the photocatalytic cleavage of the C-C σ-bond of a specific lignin model compound containing phenolic moieties with short reaction time and the visible light illumination in a HAT-DSPEC under ambient conditions.

5 Mechanistic pathways of C–C/C–O bond cleavages

Possible reaction mechanisms for the oxidation of C_α–OH and selective cleavage of C_α–C_β/C_β–O, and C_{aryl}–C_α bonds via photocatalysis were proposed. The oxidation of the secondary alcohol, C_α–OH, of a LMC (**1**) is initiated by the visible light absorption by the photocatalyst, RuC^{II} that was immobilized on the photoanode semiconductor surface, resulting in the formation of the excited state ($RuC^{II/}$*), which is sufficiently reducing to sensitize TiO_2 (**Figure 9a**). The produced RuC^{III} is then reduced to the original ground state RuC^{II} following a PECT process assisted by the NHPI/LTD pair. Oxidation of NHPI generates the active form of the co-catalyst, the PINO radical, which is thermodynamically competent to selectively abstract a hydrogen atom from the C_α of the LMC **1**. The resulting α-hydroxybenzoic radical species (**Int1**) formed after HAT catalysis undergoes a second one electron/one proton oxidation, either by the reaction with a second equivalent of phthalimide N-oxyl (PINO) or via oxidation by RuC^{III} and proton loss to the solution, resulting in the formation of the ketone product (**2**). It is worth to note that the reaction of 1 equiv. of LMC **1** at the TiO_2 photoanode requires the absorption of two-photon equivalents and the generation of 1 equiv. of product **2** and 2 equiv. of H^+ in solution. The RuC photocatalyst and NHPI/LTD co-catalyst are recovered during this photocatalysis process and can react with additional lignin equivalents following light absorption at the surface.

Possible reaction mechanisms for visible-light-driven cleavage of C_α–C_β/C_β–O bonds in a non-phenolic LMC (**3**) with RuC-TiO_2 nanoparticles (NPs) is shown in **Figure 9b**. The photoexcited RuC^{II}* formed on TiO_2 NPs under visible illumination drives charge separation by electron injection to TiO_2 NP. After electron transfer from two equiv. of RuC^{III} to the LMC **3**, the primary alcohol oxidized intermediate (**Int2**) is formed. Then, reduction of **Int2** by TiO_2(e-) or RuC^{II}* generates a ketyl radical anion species which undergoes C_β–O σ-bond cleavage to produce the cleavage intermediates **Int3** and **Int4**.[128] Then, proton transfer and retro-aldol C_α–C_β cleavage reaction

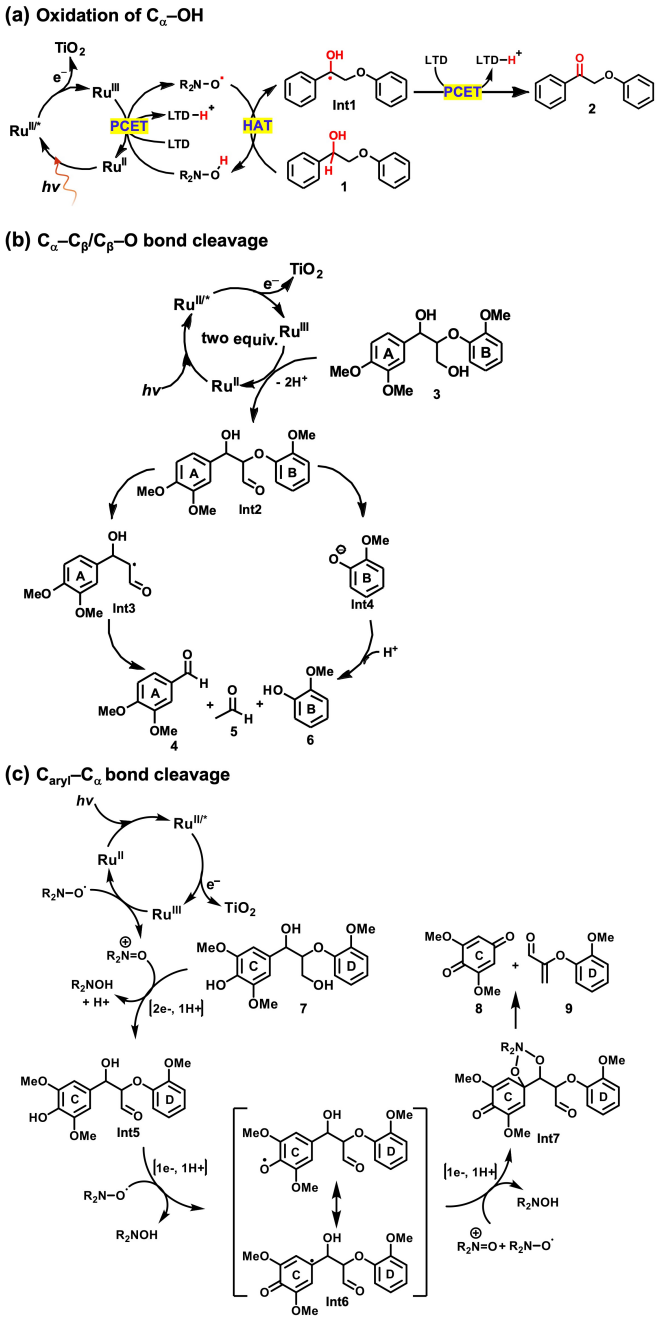

Figure 9. Proposed reaction mechanisms of (a) photo-induced chemoselective oxidation of C_α–OH in a HAT mediated DSPEC; (b) cleavage of C_α–C_β/C_β–O bonds in a non-phenolic LMC using RuC-TiO_2 NPs in the absence and presence of HAT mediator, respectively; and (c) selective cleavage of C_{aryl}–C_α bond in a phenolic LMC in a HAT coupled DSPEC cell. Reprinted with permission from references 16, 19, and 20. Copyright 2020, 2021, and 2022 American Chemical Society.

afford fragmentation products **4** and **6**. It is noted that the acetaldehyde product (**5**) was unable to detect by NMR, which could be ascribed to the evaporation of acetaldehyde during the purification process.

A unique chemical transformation pathway was observed for photocatalytic conversion of phenolic LMCs in a HAT coupled DSPEC cell, which is the cleavage of C_{aryl}–C_α bond (**Figure 9c**). After photoexcitation of the surface-bound photocatalyst RuC on the TiO_2 photoanode, the excited state RuC^{II}/* is formed, followed by the separation of electron and hole to generate TiO_2 (e^-) and RuC^{III}. Upon the hole transfer from Ru^{III} to the ACT (R_2N-O•) mediator in solution, the ground state RuC^{II} regenerates. Oxidation of R_2N-O• after hole transfer generates the oxoammonium R_2N^+=O (ACT^+) which is a strong oxidizing agent. The photochemical formation of ACT^+, and the build-up of a pool of ACT^+ near the photoanode surface then initiates a series of steps which ultimately lead to the cleavage of the C_{aryl}–C_α bond for the formation of product **8** and **9**. One equiv. of the oxoammonium likely oxidizes the primary C_γ–OH group in **8**, resulting in the formation of **Int 5**. The phenoxy radical species is then formed via a PCET process assisted by R_2N-O• (**Int6**). Upon a serial of SET process, the resulting semi-quinone intermediate is imperative to observe the products of C_{aryl}–C_α bond cleavage. It is worth to noting that LMCs that do not contain the para-hydroxyl group could not undergo such C_{aryl}–C_α bond cleavage and this leads us to infer the importance of the radical resonance form in **Int6**. The consumption of 1 eq. of R_2N-O• possibly proceeds to form the C_{aryl}–O bond in **Int7**, followed by C_{aryl}–C_α bond cleavage, reforming of R_2N^+=O, and formation of products **8** and **9**.

6 Outlook and summary

Photocatalytic and electrocatalytic biomass conversions have realized the utilization of lignin model compounds and real lignin with promising yields and selectivity. Here, the PEC process incorporated with ARM can provide the following key advantages: (i) The ability to oxidize lignin without the use of stoichiometric sacrificial oxidants, (ii) controlled lignin processing with chemical specificity through judicious choice of electrode materials and mediator catalysts, and (iii) photoelectrocatalytic oxidation under mild conditions can provide excellent selectivity for the desired oxidized products and improve existing oxidative degradation methods with complex macromolecules in the agrochemical and pharmaceutical industries. However, there are still several issues that need to be addressed. For example, the applied bias in electrocatalysis for lignin transformation needs to be minimized for excellent selective oxidative cleavage reactions. Therefore, the combination of photocatalysis and electrocatalysis for lignin depolymerization is essential to use the minimal applied bias and thereby decrease the energy cost of the system. Second, while photocatalysis could contribute to energy input for lignin reforming, it is challenging for light illumination to reach all molecules of photocatalysts in a dark-colored lignin solution, resulting in insufficient usage of solar energy in a homogeneously photocatalytic reaction for lignin conversion. Also, catalytic methods that could carry out varying chemical transformation processes in a one-pot reaction are essential for complete usage of real lignin, though several bond dissociation pathways have been reported for lignin model compounds via electrocatalysis and photocatalysis, including C_β–O, C_α–C_β, and C_{aryl}–C_α bond cleavage, respectively.[50, 128-130] Therefore, the design of a DSPEC targeting chemical transformation in lignin has considered the following: (i) fabrication of dye-sensitized photoanodes and photocathodes that could efficiently convert photon energy to electrical current, (ii) understanding the interaction between photocatalysts and mediators, (iii) overcoming the challenges of using photocatalysis in dark-colored lignin solutions, (iv) studying of the mechanism for various chemical transformations in lignin using DSPEC cells, including C_β–O, C_α–C_β, and C_{aryl}–C_α bond cleavage, and (v) finding a way to realize complete depolymerization of the inter-linked lignin with the cleavage of various C–O and C–C bonds.

Our designed DSPEC is, to our best knowledge, the first approach that uses photoelectrochemical HAT mediated catalysis to achieve visible light-driven lignin reforming in organic media. This dye-sensitized TiO_2 photoanode with HAT co-catalyst also shows promising performance for heterogeneous photo-reforming of real lignin solutions using back-side illumination of the electrode. This presents a vital step toward developing a DSPEC capable of carrying out complete lignin depolymerization. Moreover, different chemical bonds (e.g., C_β–O, C_α–C_β, and C_{aryl}–C_α) can be selectively cleaved based on the selection of the HAT co-catalysts and the structure of the LMC. The ultimate goal of this work is to selectively break down phenolic-containing biomacromolecules such as lignin to value added chemicals and biofuels, under mild conditions, with the only energy input from sunlight. Future work in the development of DSPECs for lignin conversion will focus on expanding on the combinations of photocatalysts and co-catalysts used to gain greater insight for controlling the lignin conversion pathway. In addition, developing photocathode interfaces to drive photo-reduction reactions related to lignin conversion should lead to tandem DSPEC systems that can operate without any applied electrical bias.

In summary, lignin can be selectively reformed via C–C and C–O bond cleavage to obtain value-added aromatic compounds. The selectivity is dependent on many factors, such as the use of mediators, acidic or basic conditions, chemical structures of lignin substrates, etc. Processing these chemical transformations under milder conditions (e.g., room temperature, no stoic. acids or bases) by using electrocatalysis or photocatalytic methods could preserve most of the functional structures and prevent the formation of undesired by-products, thus enhancing the selectivity and yields. Therefore, our designed mediator-assisted DSPECs for lignin degradation present a high potential to achieve excellent lignin utilization to obtain valuable chemicals.

Author Contributions

S. L.: Data Curation, Visualization, Writing – Original Draft. **S. P.:** Visualization, Writing – Reviewing & Editing. **B. D. S.:** Methodology, Validation, Reviewing. **C. G. Y.:** Conceptualization, Resources, Reviewing. **G. L.:** Supervision, Data Curation, Resources, Writing – Reviewing & Editing.

Conflicts of interest

There are no conflicts to declare.

Acknowledgements

This work was supported by the National Science Foundation grant CBET2027125 and USDA National Institute of Food and Agriculture, McIntire-Stennis program (1026723). B.D.S. thanks the Welch Foundation of Texas for support of this work through award number P-2044-2020040.

Notes

The authors declare no competing financial interest.

References

1. M. D. Kärkäs, I. Bosque, B. S. Matsuura and C. R. J. Stephenson, *Organic Letters*, 2016, **18**, 5166-5169.
2. W. Kim, E. Edri and H. Frei, *Accounts of Chemical Research*, 2016, **49**, 1634-1645.
3. M. G. Walter, E. L. Warren, J. R. McKone, S. W. Boettcher, Q. Mi, E. A. Santori and N. S. Lewis, *Chemical Reviews*, 2010, **110**, 6446-6473.
4. P. Xu, N. S. McCool and T. E. Mallouk, *Nano Today*, 2017, **14**, 42-58.
5. B. D. Sherman, M. D. Vaughn, J. J. Bergkamp, D. Gust, A. L. Moore and T. A. Moore, *Photosynthesis Research*, 2014, **120**, 59-70.
6. B. O'Regan and M. Grätzel, *Nature*, 1991, **353**, 737-740.
7. B. D. Sherman, D. L. Ashford, A. M. Lapides, M. V. Sheridan, K.-R. Wee and T. J. Meyer, *The Journal of Physical Chemistry Letters*, 2015, **6**, 3213-3217.
8. L. Alibabaei, B. D. Sherman, M. R. Norris, M. K. Brennaman and T. J. Meyer, *Proceedings of the National Academy of Sciences*, 2015, **112**, 5899-5902.
9. M. V. Sheridan, B. D. Sherman, R. L. Coppo, D. Wang, S. L. Marquard, K.-R. Wee, N. Y. Murakami Iha and T. J. Meyer, *ACS Energy Letters*, 2016, **1**, 231-236.
10. Y. Gao, X. Ding, J. Liu, L. Wang, Z. Lu, L. Li and L. Sun, *Journal of the American Chemical Society*, 2013, **135**, 4219-4222.
11. T. J. Meyer, M. V. Sheridan and B. D. Sherman, *Chemical Society Reviews*, 2017, **46**, 6148-6169.
12. B. D. Sherman, M. V. Sheridan, K.-R. Wee, S. L. Marquard, D. Wang, L. Alibabaei, D. L. Ashford and T. J. Meyer, *Journal of the American Chemical Society*, 2016, **138**, 16745-16753.
13. J. R. Swierk, N. S. McCool and T. E. Mallouk, *The Journal of Physical Chemistry C*, 2015, **119**, 13858-13867.
14. N. Klinova McMillan, D. A. Lopez, G. Leem and B. D. Sherman, *ChemPlusChem*, **n/a**, e202200187.
15. S. Li, E. W. Shuler, D. Willinger, H. T. Nguyen, S. Kim, H. C. Kang, J.-J. Lee, W. Zheng, C. G. Yoo, B. D. Sherman and G. Leem, *ACS Appl. Mater. Interfaces*, 2022, **14**, 22799-22809.
16. S. Li, U. K. Wijethunga, A. H. Davis, S. Kim, W. Zheng, B. D. Sherman, C. G. Yoo and G. Leem, *ACS Applied Nano Materials*, 2022, **5**, 948-956.
17. B. D. Sherman, N. K. McMillan, D. Willinger and G. Leem, *Nano Convergence*, 2021, **8**, 7.
18. K. A. Davis, S. Yoo, E. W. Shuler, B. D. Sherman, S. Lee and G. Leem, *Nano Convergence*, 2021, **8**, 6.
19. S. Li, U. K. Wijethunga, A. H. Davis, S. Kim, W. Zheng, B. D. Sherman, C. G. Yoo and G. Leem, *ACS Applied Nano Materials*, 2021, DOI: 10.1021/acsanm.1c03622.
20. S. Li, Z.-J. Li, H. Yu, M. R. Sytu, Y. Wang, D. Beeri, W. Zheng, B. D. Sherman, C. G. Yoo and G. Leem, *ACS Energy Lett.*, 2020, **5**, 777-784.
21. C. G. Yoo, Y. Yang, Y. Pu, X. Meng, W. Muchero, K. L. Yee, O. A. Thompson, M. Rodriguez, G. Bali, N. L. Engle, E. Lindquist, V. Singan, J. Schmutz, S. P. DiFazio, T. J. Tschaplinski, G. A. Tuskan, J.-G. Chen, B. Davison and A. J. Ragauskas, *Green Chemistry*, 2017, **19**, 5467-5478.
22. D. W. Cho, R. Parthasarathi, A. S. Pimentel, G. D. Maestas, H. J. Park, U. C. Yoon, D. Dunaway-Mariano, S. Gnanakaran, P. Langan and P. S. Mariano, *The Journal of Organic Chemistry*, 2010, **75**, 6549-6562.
23. C. M. Ha, X. Rao, G. Saxena and R. A. Dixon, *New Phytologist*, 2021, **231**, 60-74.
24. C. G. Yoo, X. Meng, Y. Pu and A. J. Ragauskas, *Bioresource Technology*, 2020, **301**, 122784.
25. E. Adler, *Wood Science and Technology*, 1977, **11**, 169-218.
26. A. Rahimi, A. Ulbrich, J. J. Coon and S. S. Stahl, *Nature*, 2014, **515**, 249-252.
27. A. D. Jodlowski, C. Roldán-Carmona, G. Grancini, M. Salado, M. Ralaiarisoa, S. Ahmad, N. Koch, L. Camacho, G. de Miguel and M. K. Nazeeruddin, *Nature Energy*, 2017, **2**, 972-979.
28. M. V. Galkin and J. S. M. Samec, *ChemSusChem*, 2016, **9**, 1544-1558.
29. Z. Sun, B. Fridrich, A. de Santi, S. Elangovan and K. Barta, *Chemical Reviews*, 2018, **118**, 614-678.
30. S. Constant, H. L. J. Wienk, A. E. Frissen, P. d. Peinder, R. Boelens, D. S. van Es, R. J. H. Grisel, B. M. Weckhuysen, W. J. J. Huijgen, R. J. A. Gosselink and P. C. A. Bruijnincx, *Green Chemistry*, 2016, **18**, 2651-2665.
31. E. Kienzle, I. Schrag, R. Butterwick and B. Opitz, *Journal of Animal Physiology and Animal Nutrition*, 2001, **85**, 148-157.
32. K. Van Aelst, E. Van Sinay, T. Vangeel, E. Cooreman, G. Van den Bossche, T. Renders, J. Van Aelst, S. Van den Bosch and B. F. Sels, *Chemical Science*, 2020, **11**, 11498-11508.
33. Y. Cao, N. Wang, X. He, H.-R. Li and L.-N. He, *ACS Sustain. Chem. Eng.*, 2018, **6**, 15032-15039.
34. T. vom Stein, T. den Hartog, J. Buendia, S. Stoychev, J. Mottweiler, C. Bolm, J. Klankermayer and W. Leitner, *Angewandte Chemie International Edition*, 2015, **54**, 5859-5863.
35. P. R. Patwardhan, R. C. Brown and B. H. Shanks, *ChemSusChem*, 2011, **4**, 1629-1636.
36. G. Zhou, P. A. Jensen, D. M. Le, N. O. Knudsen and A. D. Jensen, *Green Chem.*, 2016, **18**, 1965-1975.
37. R. K. Sharma, J. B. Wooten, V. L. Baliga, X. Lin, W. G. Chan and M. R. Hajaligol, *Fuel*, 2004, **83**, 1469-1482.
38. E. Liakakou, B. Vreugdenhil, N. Cerone, F. Zimbardi, F. Pinto, R. André, P. Marques, R. Mata and F. Girio, *Fuel*, 2019, **251**, 580-592.
39. K. Kang, R. Azargohar, A. K. Dalai and H. Wang, *Chem. Eng. J.*, 2016, **283**, 1019-1032.
40. J. Zhang, H. Asakura, J. van Rijn, J. Yang, P. Duchesne, B. Zhang, X. Chen, P. Zhang, M. Saeys and N. Yan, *Green Chem.*, 2014, **16**, 2432-2437.

41. A. Toledano, L. Serrano, A. Pineda, A. A. Romero, R. Luque and J. Labidi, *Applied Catalysis B: Environmental*, 2014, **145**, 43-55.
42. A. Rahimi, A. Azarpira, H. Kim, J. Ralph and S. S. Stahl, *Journal of the American Chemical Society*, 2013, **135**, 6415-6418.
43. R. Prado, A. Brandt, X. Erdocia, J. Hallet, T. Welton and J. Labidi, *Green Chem.*, 2016, **18**, 834-841.
44. G. Chatel and R. D. Rogers, *ACS Sustainable Chem. Eng.*, 2014, **2**, 322-339.
45. K. H. Kim, X. Bai, S. Cady, P. Gable and R. C. Brown, *ChemSusChem*, 2015, **8**, 894-900.
46. R. Lou and S.-b. Wu, *Applied Energy*, 2011, **88**, 316-322.
47. Y. Jing, L. Dong, Y. Guo, X. Liu and Y. Wang, *ChemSusChem*, 2020, **13**, 4181-4198.
48. P. J. Deuss, M. Scott, F. Tran, N. J. Westwood, J. G. de Vries and K. Barta, *Journal of the American Chemical Society*, 2015, **137**, 7456-7467.
49. S. K. Hanson, R. Wu and L. A. P. Silks, *Angew. Chem. Int. Ed.*, 2012, **51**, 3278-3278.
50. Y.-Y. Jiang, L. Yan, H.-Z. Yu, Q. Zhang and Y. Fu, *ACS Catal.*, 2016, **6**, 4399-4410.
51. R. Ma, Y. Xu and X. Zhang, *ChemSusChem*, 2015, **8**, 24-51.
52. R. Behling, S. Valange and G. Chatel, *Green Chemistry*, 2016, **18**, 1839-1854.
53. L. Ma, H. Zhou, X. Kong, Z. Li and H. Duan, *ACS Sustain. Chem. Eng.*, 2021, **9**, 1932-1940.
54. C. Yang, S. Maldonado and C. R. J. Stephenson, *ACS Catalysis*, 2021, **11**, 10104-10114.
55. L. I. Granone, F. Sieland, N. Zheng, R. Dillert and D. W. Bahnemann, *Green Chemistry*, 2018, **20**, 1169-1192.
56. I. Bosque, G. Magallanes, M. Rigoulet, M. D. Kärkäs and C. R. J. Stephenson, *ACS Central Science*, 2017, **3**, 621-628.
57. J. D. Nguyen, B. S. Matsuura and C. R. J. Stephenson, *Journal of the American Chemical Society*, 2014, **136**, 1218-1221.
58. S. Kim, S. C. Chmely, M. R. Nimlos, Y. J. Bomble, T. D. Foust, R. S. Paton and G. T. Beckham, *The Journal of Physical Chemistry Letters*, 2011, **2**, 2846-2852.
59. J. Luo, X. Zhang, J. Lu and J. Zhang, *ACS Catal.*, 2017, **7**, 5062-5070.
60. A. Perianes-Rodriguez, L. Waltman and N. J. Van Eck, *Journal of informetrics*, 2016, **10**, 1178-1195.
61. J. Chen, H. Yang, H. Fu, H. He, Q. Zeng and X. Li, *Physical Chemistry Chemical Physics*, 2020, **22**, 11508-11518.
62. X. Du, H. Zhang, K. P. Sullivan, P. Gogoi and Y. Deng, *ChemSusChem*, 2020, **13**, 4318-4343.
63. T. Shiraishi, T. Takano, H. Kamitakahara and F. Nakatsubo, 2012, **66**, 303-309.
64. M. Rafiee, M. Alherech, S. D. Karlen and S. S. Stahl, *J. Am. Chem. Soc.*, 2019, **141**, 15266-15276.
65. D. L. Ashford, M. K. Gish, A. K. Vannucci, M. K. Brennaman, J. L. Templeton, J. M. Papanikolas and T. J. Meyer, *Chemical Reviews*, 2015, **115**, 13006-13049.
66. S. Y. Reece, J. A. Hamel, K. Sung, T. D. Jarvi, A. J. Esswein, J. J. H. Pijpers and D. G. Nocera, *Science*, 2011, **334**, 645-648.
67. D. Gust, T. A. Moore and A. L. Moore, *Accounts of Chemical Research*, 2009, **42**, 1890-1898.
68. A. Fujishima and K. Honda, *Nature*, 1972, **238**, 37-38.
69. D. Duonghong, E. Borgarello and M. Graetzel, *Journal of the American Chemical Society*, 1981, **103**, 4685-4690.
70. F. E. Osterloh, *Chemical Society Reviews*, 2013, **42**, 2294-2320.
71. K. Maeda, D. Lu and K. Domen, *Chemistry – A European Journal*, 2013, **19**, 4986-4991.
72. X. Chen and S. S. Mao, *Chemical Reviews*, 2007, **107**, 2891-2959.
73. S. U. M. Khan, M. Al-Shahry and W. B. Ingler, *Science*, 2002, **297**, 2243-2245.
74. S. A. Ansari, M. M. Khan, M. O. Ansari and M. H. Cho, *New Journal of Chemistry*, 2016, **40**, 3000-3009.
75. Z. Wang, C. Yang, T. Lin, H. Yin, P. Chen, D. Wan, F. Xu, F. Huang, J. Lin, X. Xie and M. Jiang, *Advanced Functional Materials*, 2013, **23**, 5444-5450.
76. Y. Park, K. J. McDonald and K.-S. Choi, *Chemical Society Reviews*, 2013, **42**, 2321-2337.
77. K. Sivula, F. Le Formal and M. Grätzel, *ChemSusChem*, 2011, **4**, 432-449.
78. Z.-F. Huang, J. Song, L. Pan, X. Zhang, L. Wang and J.-J. Zou, *Advanced Materials*, 2015, **27**, 5309-5327.
79. Z. Li, W. Luo, M. Zhang, J. Feng and Z. Zou, *Energy & Environmental Science*, 2013, **6**, 347-370.
80. P. D. Frischmann, K. Mahata and F. Würthner, *Chemical Society Reviews*, 2013, **42**, 1847-1870.
81. M. Grätzel, *Inorganic Chemistry*, 2005, **44**, 6841-6851.
82. A. Hagfeldt, G. Boschloo, L. Sun, L. Kloo and H. Pettersson, *Chemical Reviews*, 2010, **110**, 6595-6663.
83. J. R. Swierk and T. E. Mallouk, *Chemical Society Reviews*, 2013, **42**, 2357-2387.
84. G. Leem, B. D. Sherman and K. S. Schanze, *Nano Converg.*, 2017, **4**, 37.
85. D. P. Rillema, G. Allen, T. J. Meyer and D. Conrad, *Inorganic Chemistry*, 1983, **22**, 1617-1622.
86. G. Leem, Z. A. Morseth, K.-R. Wee, J. Jiang, M. K. Brennaman, J. M. Papanikolas and K. S. Schanze, *Chemistry – An Asian Journal*, 2016, **11**, 1257-1267.
87. G. Leem, S. Keinan, J. Jiang, Z. Chen, T. Pho, Z. A. Morseth, Z. Hu, E. Puodziukynaite, Z. Fang, J. M. Papanikolas, J. R. Reynolds and K. S. Schanze, *Polymer Chemistry*, 2015, **6**, 8184-8193.
88. G. Leem, Z. A. Morseth, E. Puodziukynaite, J. Jiang, Z. Fang, A. T. Gilligan, J. R. Reynolds, J. M. Papanikolas and K. S. Schanze, *The Journal of Physical Chemistry C*, 2014, **118**, 28535-28541.
89. D. G. Brown, P. A. Schauer, J. Borau-Garcia, B. R. Fancy and C. P. Berlinguette, *Journal of the American Chemical Society*, 2013, **135**, 1692-1695.
90. K. Hanson, M. K. Brennaman, A. Ito, H. Luo, W. Song, K. A. Parker, R. Ghosh, M. R. Norris, C. R. K. Glasson, J. J. Concepcion, R. Lopez and T. J. Meyer, *The Journal of Physical Chemistry C*, 2012, **116**, 14837-14847.
91. S. A. Miller, B. A. West, A. C. Curtis, J. M. Papanikolas and A. M. Moran, *The Journal of Chemical Physics*, 2011, **135**, 081101.
92. P. G. Giokas, S. A. Miller, K. Hanson, M. R. Norris, C. R. K. Glasson, J. J. Concepcion, S. E. Bettis, T. J. Meyer and A. M. Moran, *The Journal of Physical Chemistry C*, 2013, **117**, 812-824.
93. S. Kaniyankandy, S. Verma, J. A. Mondal, D. K. Palit and H. N. Ghosh, *The Journal of Physical Chemistry C*, 2009, **113**, 3593-3599.
94. B. H. Farnum, Z. A. Morseth, M. K. Brennaman, J. M. Papanikolas and T. J. Meyer, *The Journal of Physical Chemistry B*, 2015, **119**, 7698-7711.
95. A. Yella, H. W. Lee, H. N. Tsao, C. Yi, A. K. Chandiran, M. K. Nazeeruddin, E. W. Diau, C. Y. Yeh, S. M. Zakeeruddin and M. Grätzel, *Science*, 2011, **334**, 629-634.

96. L. Zhang, X. Yang, W. Wang, G. G. Gurzadyan, J. Li, X. Li, J. An, Z. Yu, H. Wang, B. Cai, A. Hagfeldt and L. Sun, *ACS Energy Letters*, 2019, **4**, 943-951.
97. Y. Cao, Y. Saygili, A. Ummadisingu, J. Teuscher, J. Luo, N. Pellet, F. Giordano, S. M. Zakeeruddin, J. E. Moser, M. Freitag, A. Hagfeldt and M. Grätzel, *Nature Communications*, 2017, **8**, 15390.
98. J. A. Treadway, J. A. Moss and T. J. Meyer, *Inorg Chem*, 1999, **38**, 4386-4387.
99. W. J. Youngblood, S.-H. A. Lee, Y. Kobayashi, E. A. Hernandez-Pagan, P. G. Hoertz, T. A. Moore, A. L. Moore, D. Gust and T. E. Mallouk, *Journal of the American Chemical Society*, 2009, **131**, 926-927.
100. *Nature Chemical Biology*, 2011, **7**, 855-855.
101. L. Wang, L. Duan, Y. Wang, M. S. G. Ahlquist and L. Sun, *Chemical Communications*, 2014, **50**, 12947-12950.
102. D. Wang, S. L. Marquard, L. Troian-Gautier, M. V. Sheridan, B. D. Sherman, Y. Wang, M. S. Eberhart, B. H. Farnum, C. J. Dares and T. J. Meyer, *Journal of the American Chemical Society*, 2018, **140**, 719-726.
103. D. Wang, F. Niu, M. J. Mortelliti, M. V. Sheridan, B. D. Sherman, Y. Zhu, J. R. McBride, J. L. Dempsey, S. Shen, C. J. Dares, F. Li and T. J. Meyer, *Proceedings of the National Academy of Sciences*, 2020, **117**, 12564-12571.
104. S. Yun, N. Vlachopoulos, A. Qurashi, S. Ahmad and A. Hagfeldt, *Chemical Society Reviews*, 2019, **48**, 3705-3722.
105. W. J. Youngblood, S.-H. A. Lee, K. Maeda and T. E. Mallouk, *Acc. Chem. Res.*, 2009, **42**, 1966-1973.
106. Z. Yu, F. Li and L. Sun, *Energy & Environmental Science*, 2015, **8**, 760-775.
107. K.-R. Wee, B. D. Sherman, M. K. Brennaman, M. V. Sheridan, A. Nayak, L. Alibabaei and T. J. Meyer, *Journal of Materials Chemistry A*, 2016, **4**, 2969-2975.
108. B. D. Sherman, J. J. Bergkamp, C. L. Brown, A. L. Moore, D. Gust and T. A. Moore, *Energy & Environmental Science*, 2016, **9**, 1812-1817.
109. W. Song, M. K. Brennaman, J. J. Concepcion, J. W. Jurss, P. G. Hoertz, H. Luo, C. Chen, K. Hanson and T. J. Meyer, *The Journal of Physical Chemistry C*, 2011, **115**, 7081-7091.
110. M. Hambourger, P. A. Liddell, D. Gust, A. L. Moore and T. A. Moore, *Photochemical & Photobiological Sciences*, 2007, **6**, 431-437.
111. F. Li, M. Yu, Y. Jiang, F. Huang, Y. Li, B. Zhang and L. Sun, *Chemical Communications*, 2011, **47**, 8949-8951.
112. P. Farràs, C. Di Giovanni, J. N. Clifford, P. Garrido-Barros, E. Palomares and A. Llobet, *Green Chemistry*, 2016, **18**, 255-260.
113. T. V. Pho, M. V. Sheridan, Z. A. Morseth, B. D. Sherman, T. J. Meyer, J. M. Papanikolas, K. S. Schanze and J. R. Reynolds, *ACS Appl. Mater. Interfaces*, 2016, **8**, 9125-9133.
114. J. Jiang, B. D. Sherman, Y. Zhao, R. He, I. Ghiviriga, L. Alibabaei, T. J. Meyer, G. Leem and K. S. Schanze, *ACS Applied Materials & Interfaces*, 2017, **9**, 19529-19534.
115. W. Song, A. K. Vannucci, B. H. Farnum, A. M. Lapides, M. K. Brennaman, B. Kalanyan, L. Alibabaei, J. J. Concepcion, M. D. Losego, G. N. Parsons and T. J. Meyer, *Journal of the American Chemical Society*, 2014, **136**, 9773-9779.
116. D. Badgurjar, B. Shan, A. Nayak, L. Wu, R. Chitta and T. J. Meyer, *ACS Appl. Mater. Interfaces*, 2020, **12**, 7768-7776.
117. J. E. Nutting, M. Rafiee and S. S. Stahl, *Chemical Reviews*, 2018, **118**, 4834-4885.
118. H. G. Cha and K.-S. Choi, *Nature Chemistry*, 2015, **7**, 328-333.
119. D. J. Chadderdon, L.-P. Wu, Z. A. McGraw, M. Panthani and W. Li, *ChemElectroChem*, 2019, **6**, 3387-3392.
120. T. Li, T. Kasahara, J. He, K. E. Dettelbach, G. M. Sammis and C. P. Berlinguette, *Nature Communications*, 2017, **8**, 390.
121. D. F. Bruggeman, T. M. A. Bakker, S. Mathew and J. N. H. Reek, *Chemistry – A European Journal*, 2021, **27**, 218-221.
122. P. B. Pati, M. Abdellah, S. Diring, L. Hammarström and F. Odobel, *ChemSusChem*, 2021, **14**, 2902-2913.
123. S. T. Nguyen, P. R. D. Murray and R. R. Knowles, *ACS Catalysis*, 2020, **10**, 800-805.
124. S. K. Hanson, R. Wu and L. A. P. Silks, *Angew. Chem. Int. Ed.*, 2012, **51**, 3410-3413.
125. D. H. Choi, S. K. Nam, K. Jung and J. H. Moon, *Nano Energy*, 2019, **56**, 365-372.
126. X. Li, S.-M. Dai, P. Zhu, L.-L. Deng, S.-Y. Xie, Q. Cui, H. Chen, N. Wang and H. Lin, *ACS Applied Materials & Interfaces*, 2016, **8**, 21358-21365.
127. L. C. Kao, S. Y. H. Liou, C. L. Dong, P. H. Yeh and C. L. Chen, *ACS Sustainable Chemistry & Engineering*, 2016, **4**, 210-218.
128. G. Magallanes, M. D. Kärkäs, I. Bosque, S. Lee, S. Maldonado and C. R. J. Stephenson, *ACS Catalysis*, 2019, **9**, 2252-2260.
129. H. Liu, H. Li, J. Lu, S. Zeng, M. Wang, N. Luo, S. Xu and F. Wang, *ACS Catal.*, 2018, **8**, 4761-4771.
130. S. Gazi, W. K. Hung Ng, R. Ganguly, A. M. Putra Moeljadi, H. Hirao and H. S. Soo, *Chemical Science*, 2015, **6**, 7130-7142.